MC^3: A Multicharger Cooperative Charging Mechanism for Maximizing Surveillance Quality in RWSNs

Hongli Yu, Chih-Yung Chang, *Member, IEEE*, Weiguo Guan, YaJun Wang, and Diptendu Sinha Roy

***Abstract*—Recharging strategies for sensors within wireless rechargeable sensor networks (WRSNs) have emerged as a critical concern in recent years. Prior research has investigated harnessing energy from the ambient environment. However, due to environmental volatility, the reliability of such energy sources cannot be assured. Alternative approaches have used mobile chargers (MCs) to replenish energy-deficient sensors, but these methods tend to suffer from diminished efficiency in large-scale networks. This study proposes a cooperative recharging mechanism involving multiple chargers, named MC^3, which aims to equalize the workloads across MCs while concurrently minimizing sensors' recharging waiting time. The mechanism enables MCs to adjust their recharging groups based on their current positions and allows sensors to select the best MC, thus fulfilling the dual objectives of equitable workload distribution and minimization of the recharging path. The experimental study shows that the proposed algorithm outperforms the existing algorithms in terms of the waiting time of sensors, recharging effectiveness (RE), and workload balance of MCs.**

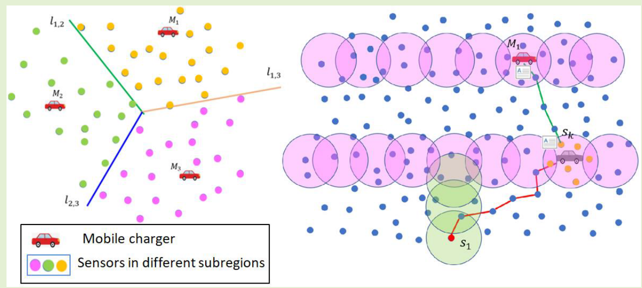

***Index Terms*— Cooperative recharging mechanisms, mobile chargers (MCs), recharging effectiveness (RE), recharging strategies, wireless rechargeable sensor networks (WRSNs).**

I. INTRODUCTION

WIRELESS sensor networks (WSNs) have been widely applied in many applications, including smart city, medical, environmental monitoring, and industrial control [1], [2], [3]. Since sensors are battery-powered, the lifetime of sensor networks is one of the most important issues in WSNs. It is very costly and difficult to charge the battery for the energy-exhausted sensors. As a result, the recharging problem of sensors has attracted the wide attention of many scholars. In literature, a large number of energy replenishment algorithms have been proposed to solve the sensor charging problem. These algorithms can be classified into two classes: energy harvesting [4], [5], [6] and wireless transfer recharging [7], [8], [9], [10], [11], [12], [13].

In the class of energy harvesting, some rechargeable devices recharge sensors by harvesting the energy from the surrounding environment, including wind and solar. However, it is impossible to provide stable energy for the WSNs due to the large uncertainty of external environmental resources. On the other hand, wireless power transfer (WPT) technology provides an effective way for energy recharging of sensors. A lot of schemes have been proposed in recent years. In the wireless transfer recharging class, the mobile charger (MC) was applied to recharge the sensors. These studies can be further divided into two categories: single-charger [7], [8], [9] and multicharger [10], [11], [12], [13].

In the class of single-charger, many studies discussed how to use the single MC to recharge the sensors by designing effective paths [7], [8], [9]. In this case, all the requested sensors were recharged by only one MC. Typically, each sensor has two energy thresholds: the recharging threshold and the sleeping threshold. In case the remaining energy reaches the recharging threshold, the recharging request will be sent from the sensor. Once the energy drops to the sleep threshold,

Manuscript received 25 February 2024; revised 25 March 2024; accepted 26 March 2024. Date of publication 8 April 2024; date of current version 15 May 2024. This work was supported in part by the Basic Scientific Research Project of the Education Department of Liaoning Province under Grant LJKMZ20220966 and in part by the Education Department of Service Local Project of Liaoning Province under Grant LJKFZ20220238. The associate editor coordinating the review of this article and approving it for publication was Prof. Guiyun Tian. *(Corresponding author: Chih-Yung Chang.)*

Hongli Yu, Weiguo Guan, and YaJun Wang are with the Department of Electronics and Information Engineering, Liaoning University of Technology, Jinzhou 121004, China (e-mail: hly@chzu.edu.cn; guanweiguo@lnut.edu.cn; wyj_lg@163.com).

Chih-Yung Chang is with the Department of Computer Science and Information Engineering, Tamkang University, Taipei 25137, Taiwan (e-mail: cychang@mail.tku.edu.tw).

Diptendu Sinha Roy is with the Department of Computer Science and Engineering, National Institute of Technology, Shillong 793003, India (e-mail: diptendu.sr@nitm.ac.in).

Digital Object Identifier 10.1109/JSEN.2024.3382887

the sensor will switch to the sleep state. Therefore, it is difficult to recharge all the requested sensors in time in the large-scale monitoring area using a single MC.

To avoid the drawbacks of the single-charger scheme, the class of multichargers developed heuristics or approximate algorithms to determine the recharging schedule and construct recharging paths accordingly.

The schemes based on multichargers focused on developing the collaborative recharging algorithm. Most existing schemes applied the heuristic or the approximate algorithm to solve the scheduling issue of multiple chargers, aiming to acquire the approximate optimal solution [10], [11], [12], [13]. Therefore, the recharging path length and workload of each MC could be reduced, and the recharging efficiency was improved.

To reduce the recharging waiting time of requested sensors, recent studies [14], [15] considered partial charging schemes. In these studies, the full recharging time can be divided into several time slots. The requested sensor can be recharged one or more time slots in each recharging cycle. Then the requested sensor will be fully recharged multiple times. These schemes have a great advantage in improving the number of recharged sensors within the given time, aiming to minimize the number of dead sensors. However, the partial recharging mechanism increases the path length of MCs, reducing the energy utilization efficiency of the MCs.

This article proposed a multicharger cooperative recharging mechanism for maximizing surveillance quality in wireless rechargeable sensor networks (WRSNs), named MC^3. Considering the large-scale WSNs, the proposed MC^3 applies multiple MCs to simultaneously recharge the sensors, aiming to balance the workload of each mobile and maintain the perpetual life of the WRSNs. Two main challenges should be considered during the design of the MC^3. First, partition the monitoring region for each MC to maximize the recharging efficiency. An efficient partition can reduce the waiting time of each requested sensor since the recharging workload can be balanced. This can further reduce the failure ratio of the sensors. To cope with this challenge, the proposed MC^3 updates the service recharging region of each MC on demand. Second, the recharging scheduling of each MC is another challenge. When the MC receives many requests from sensors, the scheduling for the recharging path and the order of requested sensors is the other important issue.

The main contributions of the proposed MC^3 are listed as follows.

1) **Achieving the Perpetual Lifetime of the WSNs.** The proposed MC^3 schedules multiple MCs to recharge the sensors, aiming to cooperatively achieve the perpetual lifetime of the WSNs.
2) **Finding the Nearest MC Automatically for All Sensors.** Different from existing studies [10], [13], the proposed mechanism enables each sensor to find the nearest MC. The proposed MC^3 dynamically constructs the shortest recharging path for MCs, instead of recharging the sensors in a cluster manner. As a result, the recharging efficiency and energy usage rate of the MC can be significantly improved.
3) **Balancing the Workloads of All MCs.** The proposed algorithm balances the workloads of all the MCs by considering the number of sensors in the recharging queue of each charger and dynamically adjusts the service region of each MC. As a result, the workloads of MCs can be balanced, which further improves the surveillance quality of the WSN.

The rest of this article is organized as follows. Section II presents the related work of recharging in WSNs. Section III describes the network environment and problem formulation. Section IV presents the proposed algorithm. Section V gives the performance evaluation. Finally, the conclusion is drawn in Section VI.

II. Related Work

In the literature, numbers of approaches apply the MC to recharge the sensors in WSNs. They can be further divided into two categories: single-charger category and multicharger category.

A. Single-Charger Category

Some existing studies fall into the single-charger category. Tomar et al. [7] proposed an on-demand scheduling algorithm for recharging sensors based on fuzzy logic. In the algorithm, the network parameters, such as the residual energy of sensors, the distance between the MC and sensor, and the density of the critical sensor, were considered as the input variables, while the scheduling probability (SP) was set to the output of the fuzzy logic. Finally, the sensor with the highest SP was considered as the next recharged object.

Guo et al. [8] designed the recharging routing based on lifespan balance. The algorithm was performed round by round. Each sensor sent the state information to the base station (BS) in each round. Based on the state information, the BS updated the multihop routing using the QoS routing algorithm. To balance the lifespan of all the sensors, the service load of low lifespan sensors was transferred by dynamically adjusting the relay range of each sensor, aiming to increase the lifespan of all the sensors.

Another study [9] proposed an efficient algorithm that integrated mobile recharging and data collection, named J-METDC, to improve the energy efficiency of the network. The spectral clustering algorithm was initially applied to partition the WSN. Then, the recharging order of the MC could be determined based on the cat swarm optimization algorithm which considered the available number of packets and residual energy. In summary, the above-mentioned studies [7], [8], [9] aimed to construct an efficient path for the MC. However, they did not consider the energy efficiency issue in a large-scale network.

B. Multicharger Category

In this category, multiple MCs were adopted to recharge the sensors deployed in the WSN. Within a certain period of time, each MC undertook the recharging task of some sensors. Therefore, how to schedule the MCs cooperatively recharging such that the energy usage can be maximized was a key issue of these approaches.

Xu et al. [10] designed the scheduling scheme for MCs from the perspective of cooperative recharging economics. This study assumed that a set of MCs were located at fixed locations in the network, and the sensors should move from their initial locations to the chargers, aiming to obtain the energy. The cost of any recharged sensor was the sum of charging cost and the movement cost. To minimize the comprehensive cost of the network, two intragroup cost-sharing schemes were presented, aiming to improve the cooperative recharging economics.

Wei et al. [11] developed a multi-MC charging schedule with time windows. It is assumed that each sensor has a recharging time window and will be recharged within the time window. When the average energy of all the sensors is lower than an upper threshold, the MC starts the recharging task. Then the multi-MC charging schedule with time windows based on a genetic algorithm was adopted to schedule the MCs, aiming to minimize the total charging cost.

Wang et al. [12] recharged the WSN through sleeping and charging schedules. When the remaining energy is lower than threshold d, they will send recharging requests to the MCs. Then a distance and energy-oriented charging scheduling algorithm was applied to schedule the recharging path for each MC.

Han et al. [13] assumed that the BS was deployed in the center of the network. A set of MCs were placed at the BS initially. The network can be divided into several uneven clusters. The cluster heads were considered as the recharging point of each MC. When the partial of sensors finished the recharging task, they acted the relay to recharge other sensors far away from the MC. Finally, the BS performed the collaborative recharging scheduling based on the energy requirement of each cluster and the distance between clusters to construct the recharging path for MCs.

Different from the studies discussed above, another study [14] proposed a partial charging scheme. This approach assumed that the sensors could be recharged partially. In addition, the efficient recharging path for each MC was constructed aiming to maximize the sum of sensor lifetimes. To improve energy efficiency, Liu et al. [15] developed a multisensor temporal spatial partial-charging algorithm, aiming to minimize the number of dead sensors.

However, most of the existing studies did not fully consider the utilization of energy. The MCs performed the recharging task for sensors within a certain area, leading to a long path length. Compared with them, the proposed MC^3 algorithm further considers the energy usage efficiency and the workload of each MC. Table I summarizes the comparisons of the related studies and the proposed MC^3.

TABLE I
COMPARISON BETWEEN ALGORITHMS

Related works	Partitioned Networks	Dynamic Scheduling	Energy Usage efficiency	Workload Balance
CCSGA[10]	○	×	×	×
MMCS [11]	×	×	○	×
DECS [12]	×	○	○	×
MCCA [13]	×	○	×	×
MSL [14]	○	○	×	×
MTSPC[15]	×	×	○	×
MC^3	○	○	○	○

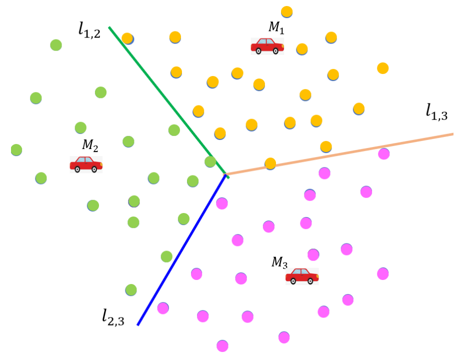

Fig. 1. Example of the considered WSNs' scenario.

III. NETWORK ENVIRONMENT AND PROBLEM FORMULATION

This section first introduces the network model and assumptions of the considered called WRSNs. Then, the problem formulation of this article is detailed.

A. Network Model

Assume that the monitoring region is R. This article considers a wireless rechargeable sensor network, which consists of a set of n sensors $S = \{s_1, s_2, \ldots, s_n\}$ randomly deployed in region R. The sensors perform the sensing and communication tasks. The data of each sensor will be collected by the sink node using multihop forwarding. Since the amount of forwarding data is different for each sensor, the energy consumption rate is different. The battery capacity of each sensor is limited, denoted by E_s. When the sensor has low remaining energy, it sends a recharging request to the MC. Upon receiving the recharging request, the MC moves to and recharges the sensor according to a recharging schedule. Since the given WRSNs might be large, one MC might not be enough to support the recharging service for all the requests sent from the sensors in the WRSN. Therefore, this article considers multiple MCs which cooperatively perform the recharging task. Let $M = \{M_1, M_2, \ldots, M_p\}$ denote the p MCs. Each MC is equipped with a wireless device, LoRa of NB-IoT, for message transmission between all the MCs. The p MCs cooperatively move at a constant speed for recharging the sensors that have sent the recharging requests.

Fig. 1 gives an example where many sensors are deployed in the monitoring region which has been partitioned into $p = 3$ subregions. The three MCs are assigned to different subregions to recharge the sensors with low energy.

B. Sensing Model

This section describes the sensing model applied in this article. The probabilistic sensing model (PSM) [16] is used in this study. The sensing range of the PSM contains two parts, the certain sensing region and the uncertain sensing region. In the certain sensing region, the event can be detected with a probability of 100%. However, when the event occurs in the uncertain sensing region, the probability of event detection changes ranging 0%–100%, depending on the distance between the location of the sensor and the event. The following equation shows the sensing probability of sensor s_i:

$$p(s_i, e\ n) = \begin{cases} 1, & d(s_i, e\ n) \le r_s^g \\ e^{-\lambda\left(d(s_i, e\ n) - r_s^g\right)^\gamma}, & r_s^g < d(s_i, e\ n) < r_s \\ 0, & d(s_i, e\ n) \ge r_s \end{cases} \quad (1)$$

where λ and γ denote the path loss exponents of the sensing signal strength and could be adjusted with the physical properties of the sensor, r_s^g and r_s represent the radii of the solid and dotted circles, respectively, and $d(s_i, en)$ is the Euclidean distance of sensor s_i and event en.

C. Energy Model

The energy model includes two parts: the energy consumption model and the energy recharging model. The following first presents the energy consumption model. Then the energy recharging model is presented. The source of energy consumption of sensors s_i depends on the operations that s_i performs. These operations include sensing, data transmitting, and forwarding. Let notations E_{sensing}, E_{tranmit}, $E_{\text{receiving}}$, and E_{forward} represent the energy consumption for sensing, packet transmitting, packet receiving, and packet forwarding, respectively, in each time slot. Let E_i^{cons} denote the energy consumption of sensor s_i in each time slot. The following equation is applied to measure E_i^{cons}:

$$E_i^{\text{cons}} = E_{\text{sensing}} + E_{\text{transmit}} + E_{\text{receiving}} + E_{\text{forward}}. \quad (2)$$

Let notations $E_{\text{th}}^{\text{request}}$ and $E_{\text{th}}^{\text{min}}$ denote the recharging and sleeping thresholds of each sensor, respectively. Let $E_i^{\text{rem},t}$ denote the remaining energy of sensor s_i at time slot t. When the $E_i^{\text{rem},t}$ is smaller than the recharging threshold $E_{\text{th}}^{\text{request}}$, sensor s_i should send a recharging request to the MC. When the remaining energy of s_i is lower than $E_{\text{th}}^{\text{request}}$, but the MC still does not recharge the sensor, the sensor should reserve minimal energy $E_{\text{th}}^{\text{min}}$ to guarantee that it can switch between sleeping and working states. Therefore, when the remaining energy $E_i^{\text{rem},t}$ is smaller than the minimal energy $E_{\text{th}}^{\text{min}}$, the sensor should switch to the sleeping state.

The following presents the recharging model of this article. Assume that each MC is aware of the locations of all the MCs and all the sensors. The network is partitioned into p subregions. Let R_i denote the ith partitioned subregion. The MC M_i is dispatched to recharge the sensors in the subregion R_i. Assume that the MC M_i is deployed in the center of the subarea R_i and is responsible for recharging those sensors in R_i.

D. Problem Formulation

This article addresses the energy replenishment problem for battery-powered WSNs. Our objective is to prolong the lifetime of WSNs by scheduling multiple MCs to recharge the sensors with low energy. The challenges of this work are illustrated in what follows. The first challenge is the cooperation issue among MCs. That is, the sensors that need to be recharged in each subregion might be different. The MCs should adaptively change their recharging subregions such that the requested sensors can reduce their waiting time and the MCs can balance the recharging workload of each MC. Second, when the MC receives many recharging requests from sensors, how to schedule its recharging task such that the recharged sensors can contribute maximal monitoring quality. The third challenge is that the location of the MC and size of each subregion might be changed. Each sensor should dynamically maintain the responsible MC and the location of that MC.

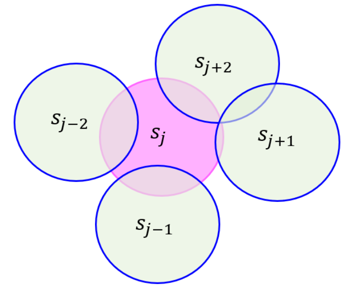

Fig. 2. Scene of several adjacent sensors.

This article aims to develop a recharging scheduling algorithm that can schedule the MCs to cooperatively recharge the sensors in a distributed manner for a given WSN. Consider a sensor s_i. Let A_i represent the coverage range of sensor s_i. In a densely deployed sensor network, the coverage range of s_i usually overlaps with its neighbors, as shown in the pink circle in Fig. 2. Let N_i denote the set of neighbors of sensor s_i. Furthermore, let N_i^{overlap} denote the set of sensors whose coverage ranges overlap with the coverage range sensor s_i. The contribution of sensor s_i can be measured by the subregion of A_i which is not overlap with the coverage ranges of any neighbor.

Let $\gamma_i^{\text{working},t}$ be a Boolean variable that represents whether or not the sensor is in working state at time slot t

$$\gamma_i^{\text{working},t} = \begin{cases} 1, & E_i^{\text{rem},t} > E_{\text{th}}^{\text{min}} \\ 0, & E_i^{\text{rem,t}} < E_{\text{th}}^{\text{min}}. \end{cases} \quad (3)$$

Let $A_i^{\text{contribute}}$ denote the coverage contribution of sensor s_i. $A_i^{\text{contribute}}$ can be measured by

$$A_i^{\text{contribute},t} = A_i \times \gamma_i^{\text{working},t} \setminus \bigcup_{s_k \in N_i^{\text{overlap}}} \left(A_k \times \gamma_k^{\text{working,t}}\right). \quad (4)$$

Let $T = \{t_1, \ldots, t_x\}$ be the monitoring period. This article aims to develop a recharging mechanism for multiple MCs such that the accumulated coverage during T is maximized. The objective of this article is presented in the following:

$$\text{Max} \sum_{t=t_1}^{t_x} \sum_{s_i \in S} A_i^{\text{contribute},t} \times \gamma_i^{\text{working},t}. \quad (5)$$

Let s_i^{state} denote the state of sensor s_i, which has three possible modes, including strong working, weak working, and sleeping modes.

Definition 1: Let three Boolean variables δ_i^{SW}, δ_i^{WW}, and δ_i^{SL} represent the strong working, weak working, and sleeping states, respectively.

Strong Working State: When the remaining energy $E_i^{\text{rem},t}$ of sensor s_i is higher than the recharging threshold $E_{\text{th}}^{\text{request}}$, sensor s_i should stay in a strong working state.

Weak Working State: In case that the remaining energy $E_i^{\text{rem},t}$ of sensor s_i satisfies the condition

$$E_{\text{th}}^{\text{min}} < E_i^{\text{rem},t} < E_{\text{th}}^{\text{request}}$$

sensor s_i should stay in a weak working state.

Sleeping State: Once the remaining energy $E_i^{\text{rem},t}$ of sensor s_i is lower than the minimal energy $E_{\text{th}}^{\text{min}}$, sensor s_i should stay in the sleeping state.

The state s_i^{state} of δ_i^{SW}, δ_i^{WW}, and δ_i^{SL} can be expressed as follows:

$$\delta_i^{SW} = \begin{cases} 1, & \text{if } s_i^{\text{state}} = \text{Strong Working} \\ 0, & \text{otherwise} \end{cases} \tag{6}$$

$$\delta_i^{WW} = \begin{cases} 1, & \text{if } s_i^{\text{state}} = \text{Weak Working} \\ 0, & \text{otherwise} \end{cases} \tag{7}$$

$$\delta_i^{SL} = \begin{cases} 1, & \text{if } s_i^{\text{state}} = \text{Sleep} \\ 0, & \text{otherwise.} \end{cases} \tag{8}$$

Some constraints given below must be satisfied to achieve the objective of this article. The following state constraint means that each sensor must stay in one of the three working states in any time slot. Equation (9) expresses the state constraint.

State Constraint

$$\delta_i^{SW} + \delta_i^{WW} + \delta_i^{SL} = 1, \quad \text{for } \forall s_i \in S. \tag{9}$$

Let Boolean variables $\mu_{i,j}$ represent whether or not sensor s_j is being recharged by a MC M_i at slot t. That is,

$$\mu_{i,j}^t = \begin{cases} 1 \text{ if } s_j \text{ is being recharged by } M_i \text{ at slot } t. \\ 0 \qquad\qquad \text{otherwise} \end{cases} \tag{10}$$

The sensor recharging constraint presents that any sensor s_j can be recharged by at most one MC at any time slot t.

Sensor Recharging Constraint

$$\sum_{i=1}^{p} \mu_{i,j}^t \le 1. \tag{11}$$

Equation (12) gives the constraint that each MC can only recharge for at most one sensor in each recharging time slot t. The following MC recharging constraint reflects this requirement.

MC Recharging Constraint

$$\sum_{j=1}^{n} \mu_{i,j}^t \le 1. \tag{12}$$

Let μ_i^t denote whether or not an MC M_i is charging sensor s_j at time slot t. It is obvious that the MC can recharge at most one sensor at a time. That is,

$$\mu_i^t = \sum_{j=1}^{n} \mu_{i,j}^t.$$

Let T^{round} denote a recharging cycle which represents the period time from the time point that the MC leaves from the BS to the time point it returns to the BS. Let β^{chg} and β^{mov} represent the energy consumption rates for MC recharging and moving, respectively. The energy consumption sources of the MC mainly consist of recharging and moving. Let E_M denote the battery capacity of the MC. The sum of the energy consumed by the MC for recharging sensors and walking must be less than the battery capacity of the MC in a cycle. The MC energy constraint guarantees that the energy consumption of an MC M_i in a recharging cycle is smaller than its battery capacity.

MC Energy Constraint

$$\sum_{t=1}^{T^{\text{round}}} \left(\mu_i^t * \beta^{chg} + \left(1 - \mu_i^t\right) * \beta^{\text{mov}} \le E_M \,. \tag{13}$$

Section IV presents the proposed algorithm which aims to achieve the goal of this article and satisfy the constraints in (9)–(13).

IV. Proposed Algorithms

This section presents the proposed charging algorithm MC^3 which aims to maximize the surveillance coverage of the given monitoring region. The proposed MC^3 mainly consists of the network initialization phase, recharging groups adjusting (RGA) phase, sensor recharging request phase, and recharging schedule and workload balancing phase. The network initialization phase aims to partition the monitoring region into p groups and then assign one group to one MC. The RGA phase aims to adjust the recharging group dynamically to reduce the recharging path length and shorten the waiting time. Since the location of each MC is changed with time, the sensor recharging request phase aims to select the nearest MC and send the recharging request message to it. Finally, the recharging schedule and workload balancing phase aim to construct the recharging path while balancing the workload of each MC.

A. Network Initialization Phase

In this phase, the network initialization task is performed. The major task includes the network partitioning and position initialization of MCs. The following presents the details of each step.

Step 1: Network Partitioning

This step aims to partition the considered monitoring region into several subregions according to the location of sensors. Let $A_{M,N}$ denote the 2-D monitoring area with n deployed sensors, where M and N represent the length and width of the region, respectively. Let $l_i^s = (x_i^s, y_i^s)$ represent the location of sensor s_i. In this step, the k-means clustering algorithm is applied to partition the sensors in R. The region R will be partitioned into m subregions. The following presents the details of the network partitioning task.

1) Selecting m sensors from S. Let $\hat{S} = \{\hat{s}_1, \hat{s}_2, \ldots, \hat{s}_m\}$ represent the set of selected m sensors. Initially, each $\hat{s}_i \in \hat{S}$ will form a group G_i. Let (x_c^i, y_c^i) denote the center of gravity of each group G_i. The initial value of (x_c^i, y_c^i) is (x_i^s, y_i^s).

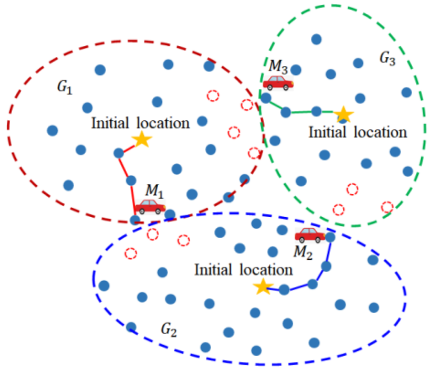

Fig. 3. Example of MCs moving to the boundary of the groups.

2) Let d_{s_i,s_j} denote the distance between s_i and s_j. The value of d_{s_i,s_j} can be calculated by applying the following equation:

$$d_{s_i,s_j} = \left[\left(x_i^s - x_j^s\right)^2 + \left(y_i^s - y_j^s\right)^2\right]^{1/2}. \quad (14)$$

Each sensor $s_j \notin \hat{S}$ should calculate its distance to each sensor $\hat{s}_i \in \hat{S}$. Let $s_{s_j,\hat{s}_i}^{\text{shortest}}$ denote the closest sensor $\hat{s}_i \in \hat{S}$ to sensor s_j. The $s_{s_j,\hat{s}_i}^{\text{shortest}}$ can be obtained by applying the following equation:

$$s_{s_j,\hat{s}_i}^{\text{shortest}} = \arg d_{s_j,\hat{s}_i}. \quad (15)$$

Then sensor s_j will become a member of the group G_i. According to the above-mentioned rule, all the sensors can be divided into m groups.

3) The center of gravity, denoted by (x_c^i, y_c^i), of each group G_i can be calculated by the following equation:

$$\left(x_c^i, y_c^i\right) = \left(\frac{\sum_{s_j \in G_i} x_j}{|G_i|}, \frac{\sum_{s_j \in G_i} y_j}{|G_i|}\right). \quad (16)$$

4) Repeat the operations 1)–3) until the member in each group is unchanged. The next step aims to initialize the location of each MC M_i to recharge the sensors in each group G_i.

Step 2: Position Initialization of MCs

Each sensor group G_i will be assigned with a mobile charge, M_i. At the beginning, each sensor is fully recharged and performs the sensing and data transmission tasks with sufficient power. The MC M_i initially moves counterclockwise spiral to the sensor, whose location is closest to the center of the group G_i, to perform the recharging task. Fig. 3 shows an example of MCs moving to the boundary of the groups.

B. RGA Phase

This phase aims to dynamically adjust the groups $G_i (1 \leq i \leq m)$ to enhance the recharging efficiency. The RGA phase will be performed whenever the MC finishes the recharging task for one requested sensor. Recall that each MC is responsible for one group of sensors. It is possible that the MCs move to the boundary of the group. This might result in a situation in which some MC is closer to the sensors of the neighboring group but is far away from most sensors in their group. This might lead to long recharging path which consumes the energy of the MC and increases the waiting time for the sensor to be recharged. To avoid this situation, this phase dynamically adjusts the recharging group of each MC to ensure that the requested sensors can send recharging requests to the closest MC. Fig. 3 shows an example of the above-mentioned scenario. The requested sensors are marked with red. As shown in Fig. 3, MC M_1 moves to the boundary of G_1, which causes the situation that the requested sensors in G_2 are closer to M_1 than M_2. Similarly, the requested sensors in G_3 are closer to M_2 than M_3. Obviously, it will increase the recharging path length if M_2 and M_3 are still responsible for recharging the requested sensors in G_2 and G_3, respectively. To shorten the path length, the service range of each MC must be dynamically changed such that M_1 has opportunities to recharge the sensors in G_2. Therefore, this phase reconstructs the service range for each MC dynamically. To achieve this, the Voronoi diagram is applied. The following gives the operations for dynamically changing the service range of each MC.

1) Let $l_i^M = (x_i^M, y_i^M)$ represent the location of MC M_i. Let the L_{M_i,M_j} represent the line segment from M_i to M_j. The segment between the adjacent MC can be represented as

$$L_{M_i,M_j} = \left(l_i^M, l_j^M\right).$$

2) Let $l_{i,j}$ denote the mid-perpendicular line of the segment L_{M_i,M_j}. For each pair of neighboring MCs, say M_i and M_j, derive the mid-perpendicular line. The $l_{i,j}$ can be calculated by applying the following equation:

$$l_{i,j} = -\frac{x_j^M - x_i^M}{y_j^M - y_i^M} \times \left[x - \frac{x_i^M + x_j^M}{2}\right] + \frac{y_j^M + y_i^M}{2}. \quad (17)$$

3) These mid-perpendicular lines will play the role of Voronoi edges and form a Voronoi diagram. The new service range of each MC M_i will be represented as the range of Voronoi cell. Let G_i' denote the new recharging group of MC M_i.

Fig. 4 depicts an example of service range adjustment for three MCs. Consider MC M_1. The area of the new recharging group of M_1 is formed by edges $l_{1,2}$ and $l_{3,1}$, as shown in Fig. 4. This phase can achieve at least the following two advantages.

1) Advantage of RNC: This phase can guarantee that the sensors will send the recharging request to the nearest MC, rather than the MC in its group. Therefore, the waiting time of the requested sensor can be reduced significantly. Fig. 5 shows an example of this advantage. The recharging group of each MC in the last round is marked with black lines while the requested sensors are marked with red. As shown in Fig. 5, when the remaining energy of s_1 is lower than the recharging threshold, s_1 will send the recharging request to the MC M_2, rather than M_1. Similarly, the same situation can be found as shown in sensor s_6. Therefore, the requested sensor can be recharged earlier, improving the coverage ratio.

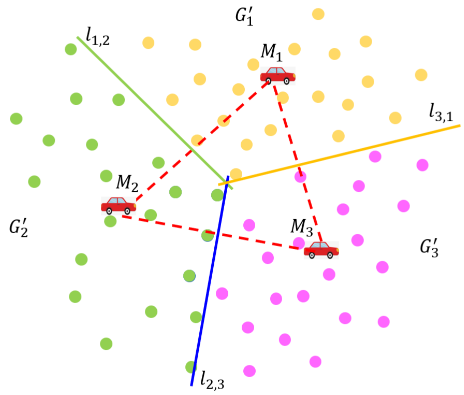

Fig. 4. Example of service range adjustment of three MCs.

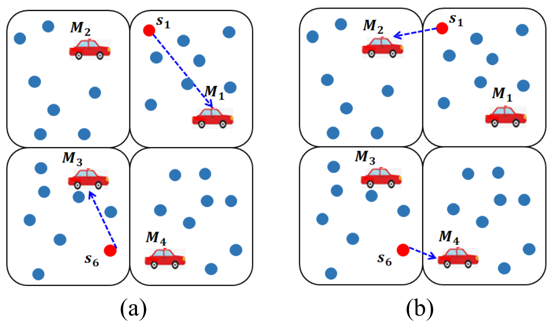

Fig. 5. Recharging distance (RNC). (a) Without applying RGA phase. (b) Applying RGA phase.

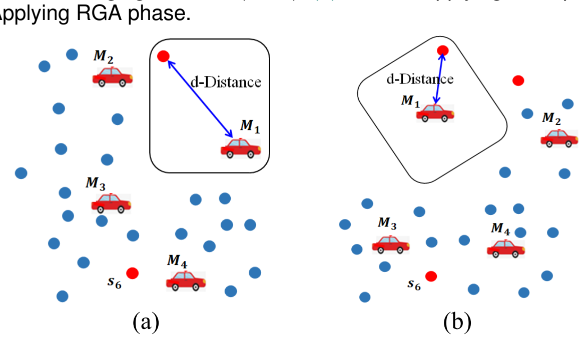

Fig. 6. Recharging distance (SDD). (a) Without applying RGA phase. (b) Applying RGA phase.

2) Advantage of SDD: Let d denote the distance between the MC M_i to the farthest recharged sensor in the recharging group of M_i. This group is called the d-distance group. Fig. 6 shows the difference in applying or not applying the proposed RGA phase. As shown in Fig. 6(b), the proposed RGA phase can generally shorten the recharging path length of the requested sensors.

C. Sensor Recharging Request Phase

This phase aims to help the sensor that has low energy to find the nearest MC, aiming to send the recharging requests to the nearest MC. This phase consists of two tasks: Location information broadcasting and recharging request message transmission. In what follows, the details of the two tasks are presented.

Task 1: Location Information Broadcasting

Since the MC performs the recharging task along the recharging path, the location of each MC is changed with time. This makes it difficult for the sensors to be aware of the locations of MCs. To ensure that the requested sensors can obtain the up-to-date location information of MCs, each MC should broadcast the location information to the surrounding sensors when the MC reaches a new location. To avoid message flooding, this task further addresses two problems: the location broadcast of MCs and the information exchange between sensors.

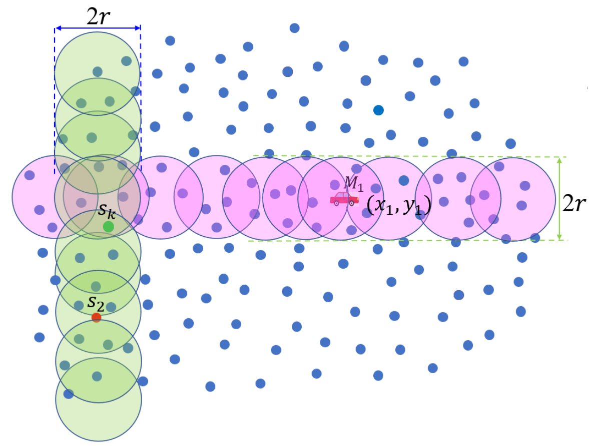

Fig. 7. Location broadcast method of M_1.

1) For the MCs

Recall that the location of MC M_i is represented as $l_i^M = (x_i^M, y_i^M)$. Let r denote the communication radius of the MC. The quorum system will be adopted to avoid message flooding. The location information of the MC is transmitted by the MC M_i in the horizontal direction within the diameter of $2r$. The sensor s_j that receives the message should check whether its location satisfies the following horizontal tubule rule.

Horizontal Tubule Rule

$$y_i^M + r \le y_j^S \le y_i^M - r. \tag{18}$$

If it is the case, the sensor will maintain the location of MC M_i and then rebroadcast the message to the neighboring sensors. On the contrary, if it is not the case, the sensor will simply drop the message without doing any operation. Let $S_{M_i,t}^{\text{horizon}}$ denote the set of sensors which maintain the location information of MC M_i at time t. When the MC arrives at a new location, it will broadcast its new location (x_i^M, y_i^M). The sensors that cooperatively broadcast the message of (x_i^M, y_i^M) will form a tubule with a radius of r.

Fig. 7 gives an example of the location broadcast of MC M_1. As shown in Fig. 7, MC M_1 transmits its location information in the horizontal direction. The sensors within the pink tubule can receive the location information of M_1 and maintain up-to-date location information. Obviously, the sensors outside the pink tubule will not be able to obtain the location information of M_1.

2) For the Request Sensors

When the remaining energy of sensor s_j reaches the recharging threshold $E_{\text{th}}^{\text{request}}$, it needs to know the location of the nearest MC. Therefore, sensor s_j sends the location inquiry message to its neighbors. Upon receiving the location inquiry message, the neighboring sensor should check whether its location satisfies the following vertical tubule rule.

Vertical Tubule Rule

$$x_i^M + r \leq x_j^S \leq x_i^M - r. \quad (19)$$

If it is the case, it will broadcast the location inquiry message to the neighbors. Let $S_{M_i,t}^{\text{vertical}}$ denote the set of sensors that satisfy the vertical tubule rule. The sensors in $S_{M_i,t}^{\text{vertical}}$ will form a vertical tubule with a radius r. Since the vertical and horizontal tubules must have at least one intersection, the sensors $s_k \in S_{M_i,t}^{\text{horizon}} \cap S_{M_i,t}^{\text{vertical}}$ can reply with the location $l_i^{M_i}$ of MC M_i to the requested sensor s_j along the vertical tubule. As shown in Fig. 5, the vertical tubule is marked with green. When sensor s_2 sends the location inquiry message to the sensors in the green tubule, it will receive the location of M_1 from sensor s_k.

Assume that p MCs are deployed in the monitoring area. Sensor s_j sends the location inquiry message in the vertical direction at time slot t. Then s_j will receive p locations of MCs. Finally, the distance between s_j and each MC can be calculated by applying (14), and the MC closest to s_j will be selected to perform the recharging task for the sensor s_j.

Task 2: Recharging Request Message Transmission

In the last task, a sensor, say s_j, with low energy can apply the quorum system to obtain the locations of all the MCs and select one that is closest to the sensor. In this task, the sensor s_j which has low remaining energy aims to send the recharging request to the nearest MC. Once the recharging MC is selected, the requested sensor s_j will send the recharging request to that MC. The location-aware routing protocol [17] is used to transmit the recharging request for the sensors. Let N_j denote the set of neighbors of sensor s_j. Recall that $l_j^s = (x_j^s, y_j^s)$ and $l_i^M = (x_i^M, y_i^M)$ represent the locations of sensor s_j and the closest MC M_i. The location-aware route can be constructed as the descriptions in what follows. The sensor s_j will transmit its recharging request to its neighbor s^{best} which satisfies the following rule:

$$s^{\text{best}} = \arg\min_{s_k \in N_j} d_{s_k, M_i}. \quad (20)$$

Upon receiving the recharging request from s_j, the sensor s^{best} will forward this request to its neighbor which satisfies (20). As a result, the recharging request will be forwarded to MC M_i along the shortest path.

Fig. 8 depicts an example where sensor s_1 transmits a recharging request to the closest MC M_1. Initially, sensor s_1 identifies the best forwarder s_3 from its neighbor by applying (20)

$$s_3 = \arg\min_{s_k \in N_1} d_{s_k, M_1}.$$

Then, sensor s_1 transmits a recharging request to s_3. Upon receiving this request message, sensor s_3 further forwards this request to its neighbor s_8 by applying the following calculation:

$$s_8 = \arg\min_{s_k \in N_3} d_{s_k, M_1}.$$

The message can be forwarded step by step until it arrives M_1.

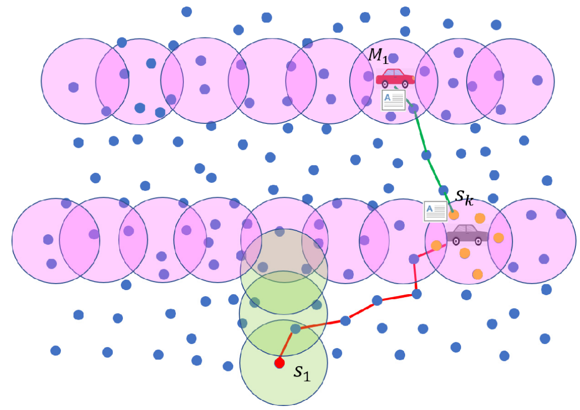

Fig. 8. Route of a request message from s_1 to M_1.

It is possible that the MC finishes its recharging task before receiving the request message sent from s_i. Then the MC might leave its current location $l_i^M = (x_i^M, y_i^M)$, aiming to go to the next sensor to execute the recharging task. To guarantee that the message sent from sensor s_i can be successfully delivered to M_i, the MC M_i should broadcast the state information to the neighboring sensors which are located within the tubule. The state information includes the next stop location of sensor, say s_{next}, moving speed v and the expected arrival time t_{arrive}. Let $S_{M_i,t}^{\text{state}}$ denote the set of sensors that received the state information from M_i. Once the request message of sensor s_i is received by sensors in the set $S_{M_i,t}^{\text{state}}$, the sensor which has the largest ID in the set $S_{M_i,t}^{\text{state}}$ will be responsible for forwarding the message to M_i. Continue to the example shown in Fig. 7, assume that mobile charger M_1 finishes the current recharging task and moves from $l_1 = (x_1, y_1)$ to another location $l_2 = (x_2, y_2)$ for recharging another sensor. However, the new location l_2 still has not updated to s_1. According to the old location information of M_1, sensor s_1 will send a message to M_1. This message will be forwarded to the sensors near the location l_1 along the red route as shown in Fig. 8. As a result, the message of s_1 cannot be received by M_1. To cope with this problem, the surrounding sensors of l_1, say sensor $s_k \in S_{M_i,t}^{\text{state}}$, will forward the request message of s_1 to M_1 along the green route as shown in Fig. 8, by applying the location-aware routing algorithm.

D. Recharging Schedule and Workload Balancing Phase

This phase consists of two tasks: recharger scheduling task and workload balancing task. To improve the recharging efficiency, the MC performs the first task, aiming to schedule the recharging path according to the request message maintained in the buffer of each MC. Then the MC performs the second task, aiming to balance the workload of each MC by adjusting the number of service sensors.

Task 1: Recharger Scheduling

In this task, the recharging path of MC M_i is constructed for recharging the requested sensors in the group G_i. According to the location and urgency of the requested sensors, the MC schedules the order of the sensors in the recharging path according to the request sensors in the queue and the newly received requests. The MC reschedules the recharging path for the newly received requests which can contribute to more surveillance quality. The recharging path construction and dynamic adjustment strategy can refer to the algorithm proposed in the previous study [18].

Task 2: Workload Balancing

This task aims to balance the workload of each MC. Let $r_{i,j} = (s_j, t_j, \text{loc}(s_j))$ represent the request message sent from s_j to M_i, where t_j and $\text{loc}(s_j)$ represent the maximum remaining working time and the location of s_j, respectively. Let $R_i = \{r_{i,1}, r_{i,2}, \ldots, r_{i,|R_i|}\}$ represent the recharging requests in the buffer of MC M_i. Each MC measures its own recharging load in the past ρ days. The MCs can directly exchange their locations and workload information through wireless technologies such as LoRa of NB-IoT. Therefore, the quorum sensors will receive both the location and workload information of each MC. For load balancing, the sensor does need not to send the recharging request to the assigned MC. Consider the sensor s_k which belongs to the group G_i. Sensor s_k will consider both the distance $d(s_k, M_i)$ and the recharging workload of each MC comprehensively, aiming to balance the workload of all the MCs. Then the recharging request will be sent to the most fit MC. The following introduces how sensor s_k selects the MC.

Let MC M_j be the geographical neighbor of M_i. To balance the workloads of all the MCs, the neighboring MC M_j will cooperate with M_i to balance their workload by sharing the requested sensors and constructing the recharging path. For the sensor s_k, when the workload of the nearest MC is too much in the past day, s_k will send the recharging request to the other MC with a low workload and a longer distance. However, the distance between s_k and the new MC must satisfy the shortest distance rule.

The shortest distance rule aims to balance the workload among MCs but guarantees that the requested sensor s_k will not increase a large overhead in terms of path length.

Shortest Distance Rule

$$\left[d\left(s_k, M_i\right) - \left(s_k, M_j\right)\right] < \varphi \tag{21}$$

where φ is a predefined threshold value.

In case the above-mentioned rule is satisfied, the workload balancing task can be performed by each requested sensor.

V. Performance Evaluation

This section evaluates the performance of the proposed MC^3 against the existing works CAERM [18] and CSGP [19]. The CAERM algorithm aimed to maximize the surveillance quality of the given networks by considering the coverage contribution of each requested sensor. The CSGP [19] algorithm assumed that the BS could receive the recharging request from each sensor and could communicate with the MVCs. The BS determined the schedule path and recharging times of the halting positions for each MVC by applying the NSGA-II and AHP-TOPSIS algorithms. In the experimental study, we used MATLAB 2021 as the simulation tool. The following shows the simulation model and discusses the simulation results.

A. Simulation Model

Assume that a set of rechargeable sensors have been deployed over the 500×500 m monitoring region and there are five MCs in the region, as shown in Fig. 9. The number of MCs depends on the number of monitoring subareas. That is, each monitoring subregion R_i is assigned with an MC. When the sensor's remaining energy is lower than the 720J, it will send the recharge request to the nearest MC. The communication distance of each sensor and MC is set at 2 m. The recharging and discharging rates of the battery are set at 2 and 0.1 J/s, respectively. The MC moves at a speed of 2 m/s. Table II lists the simulation parameters used in this article. The values of partial parameters are referred to studies [20] and [21].

TABLE II
Simulation Parameters

Parameter	Value
Network Size	500m×500m
Number of Sensors	500-1000
Density Degree	1-5
Communication Radius	2m
Number of Mobile Chargers	5-10
Speed of M	2-10m/s
Battery capacity	10KJ
Recharging Rate	2J/s
Discharging Rate	0.1-0.4J/s
Sleep threshold	20J-80J
Sensing range	10m-50m

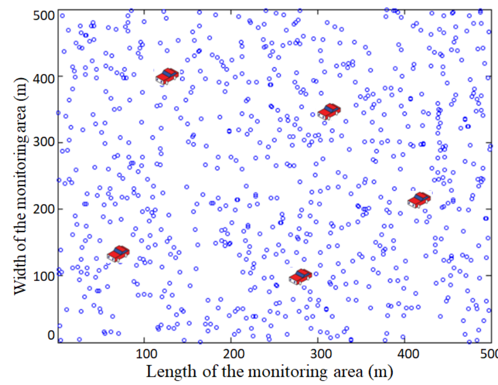

Fig. 9. Scenario that sensors are deployed environment.

B. Simulation Results

Fig. 10 shows comparison of the proposed MC^3 and the existing two algorithms in terms of coverage ratio. The coverage ratio can be defined as the size of the area covered by active sensors in the monitoring region divided by the size of the whole monitoring region. As shown in Fig. 10, the coverage is increased with the sensing range. This occurs because the larger sensing range leads to a larger coverage area. Fig. 10 also shows the impact of the sleep threshold of the sensor. Since a small sleep threshold results in a long sensing time, the coverage ratio is decreased with the sleep threshold. In comparison, the proposed MC^3 outperforms the other two methods, in terms of the coverage ratio. The reasons are stated in the following. After the MC moves to a sensor and finishes the recharging task, it will redefine its serving region and notify the sensors in this region such that sensors in the recharging region are closest to the MC. The new serving region is defined based on the concept of the Voronoi diagram. This makes sure that each sensor can

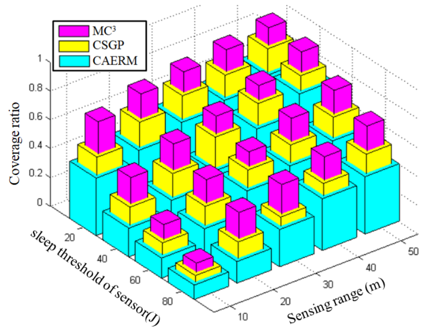

Fig. 10. Performance comparison of the MC^3, CAERM, and CSGP algorithms in terms of coverage ratio.

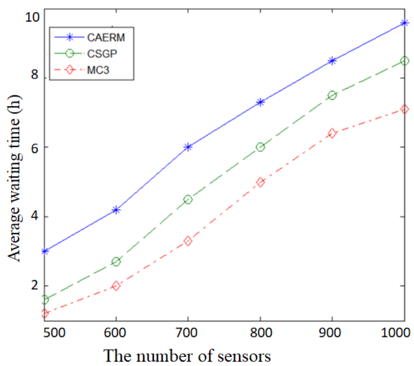

Fig. 11. Performance comparison of the proposed MC^3, CAERM, and CSGP algorithms in terms of average waiting time.

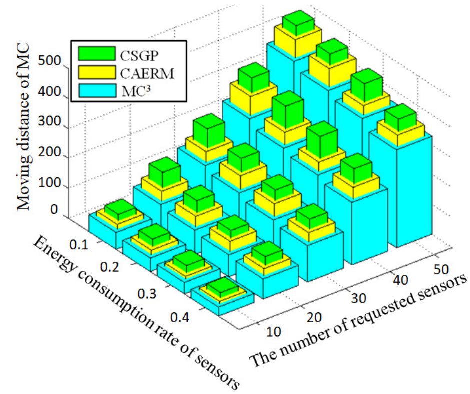

Fig. 12. Performance comparison of MC^3, CAERM, and CSGP in terms of moving distance by varying the energy consumption rate and the number of requested sensors.

send its recharging request to the closest MC. Therefore, the proposed mechanism reduces the recharging path length. As a result, each recharging requested sensor can reduce the waiting time for recharge, increasing the coverage ratio. The CAERM establishes a recharging path by considering the urgency of the requested sensor and the impact on the waiting time of other nodes. However, this policy might lead to a long recharging path. The CSGP aimed to recharge the requested sensors using a multinode recharging scheme. However, it is difficult to satisfy the energy request of each sensor. As a result, MC^3 achieves the best performance, compared with the CAERM and CSGP algorithms.

Fig. 11 shows comparison of the proposed MC^3 with the other two algorithms in terms of the average waiting time for full recharge. The number of sensors varies ranging from 500 to 1000. Let notation t_i^{wait} denote the waiting time of sensor s_i. Let $\bar{p} = \{s_0, s_1, \ldots, s_i, \ldots, s_N\}$ represent the recharging path of MC M^k at the current recharging cycle. The MC moves starting from sensor s_0. Let t_i^{ch} denote the recharging time of sensor s_i. Then the waiting time of sensor s_i can be calculated by applying the following equation:

$$t_i^{\text{wait}} = \sum_{i=1}^{N-1} t_i^{ch} + \left(\sum_{i=0}^{N-1} d\left(s_i^{\bar{p}}, s_{i+1}^{\bar{p}}\right) \right) \Big/ v \tag{22}$$

where $d(s_i^{\bar{p}}, s_{i+1}^{\bar{p}})$ denotes the distance between the sensor s_i and s_{i+1} in path $\bar{p}$ and v is the moving speed of M^k. Furthermore, the average waiting time for full recharge is

$$t_{M^k,\bar{p}}^{\text{aver\_wait}} = \frac{\sum_{i=0}^{|\bar{p}|} t_i^{\text{wait}}}{|\bar{p}|}. \tag{23}$$

Fig. 11 shows the trend that the average waiting time for the full recharge is increased with the number of sensors in the monitoring area. This occurs because the number of the requested sensor will be increased when a larger number of sensors are deployed in the monitoring area. In comparison, the proposed MC^3 outperforms the CSGP and CAERM algorithms. It occurs because MC^3 adjusts the service range dynamically. Then the MC constructs the recharging path to achieve the goal that each sensor can be recharged by the nearest MC. Finally, the waiting time of sensors is shorter than those of the other two compared algorithms.

Fig. 12 shows comparison of MC^3, CSGP, and CAERM in terms of the moving distance of MC. The number of requested sensors varies ranging from 10 to 50 while the energy consumption rate of sensors varies ranging from 0.1 to 0.4. It is observed that the compared three algorithms have a similar trend in that the recharging path lengths are increased with the number of requested sensors. This occurs because the increasing number of requested sensors will increase the recharging path. On the other hand, a large energy consumption rate can lead to a larger number of energy recharging requests from sensors. That is, the MC will receive more recharging requests at a certain time, leading to a longer recharging path length. In comparison, the proposed MC^3 outperforms the CSGP and CAERM algorithms in terms of the moving distance of MCs. This occurs because the MC adjusts its severing area dynamically. This makes sure that sensors in this area are closest to the charger and helps timely reduce the distance between each sensor and the new MC. As a result, the recharging path length of the proposed MC^3 is shorter than that of CSGP and CAERM.

Fig. 13(a) shows comparison of the three algorithms in terms of energy usage index by varying the density degree and the elapsed time. The energy usage index is defined as the total energy obtained by the requested sensors divided by the total consumption energy. The density degree represents the density of the deployed sensors and the degree varies ranging from 1 to 4.

Let η denote the energy usage index of MCs. Let notations E_M^{charge} and E_M^{move} denote the recharging energy and moving energy consumption of each MC. Then the energy usage index

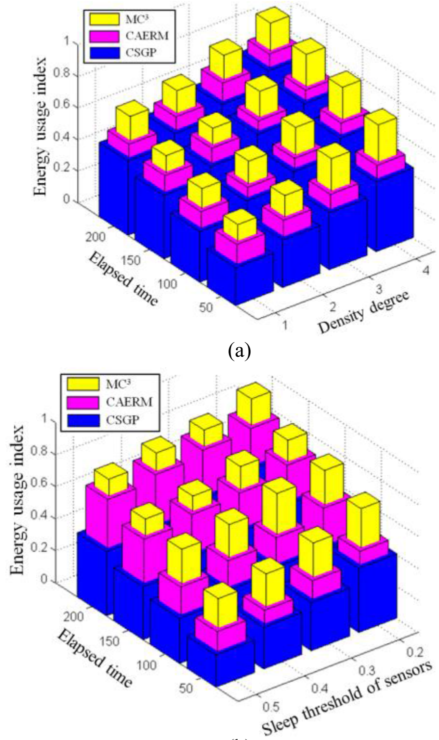

(a)
(b)

Fig. 13. (a) Comparisons of the three algorithms in terms of energy usage index by varying the elapsed time and the density degree. (b) Comparisons of the three algorithms in terms of energy usage index by varying the elapsed time and the sleep threshold of sensors.

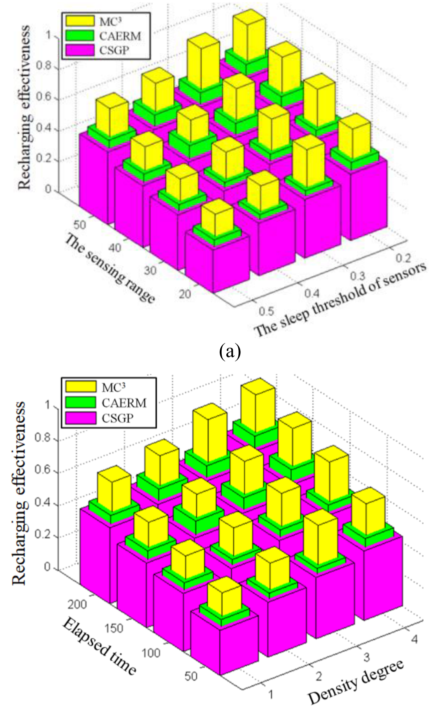

(a)
(b)

Fig. 14. (a) Performance comparisons of MC^3, CAERM, and CSGP in terms of RE by varying the sleep threshold and the sensing range of sensors. (b) Performance comparisons of MC^3, CAERM, and CSGP in terms of RE by varying the elapsed time and the density degree.

can be calculated by

$$\eta = \frac{E_M^{\text{charge}}}{E_M^{\text{charge}} + E_M^{\text{move}}}. \tag{24}$$

As shown in Fig. 13(a), the energy usage index of the three compared algorithms is increased with the density degree. In case that the density degree of sensors increases, the average distance between requested sensors will be reduced, leading to a larger value of energy usage index. On the other hand, the energy usage index of the three algorithms increases with the elapsed time. This occurs because more sensors will be recharged when the elapsed time grows. In general, the proposed MC^3 achieves better performance than the other two compared algorithms. Since the CAERM recharges all the requested sensors in each subregion with a fixed MC, the scenario shown in Fig. 3 may occur frequently, leading to more energy consumed by the MC. The reasons are presented in what follows. In CSGP, the MC performs the recharging task when it stops at the halting point, and the recharging time at each halting point is decided by a partial recharging timer. However, for the sensors to achieve a full recharge, several recharging cycles are required, which leads to a low energy usage index. Consequently, MC^3 outperforms CSGP in terms of the energy usage index.

Fig. 13(b) further shows comparison of the energy usage index of the three algorithms by varying the sleep threshold. As shown in Fig. 13(b), the compared algorithms have a similar trend in that their energy usage indices are decreased with the sleep threshold. This occurs because the small sleep threshold means that a sensor can be recharged with more energy in each recharging task, leading to a higher value of η. In comparison, the MC^3 outperforms the CAERM and CSGP algorithms. This occurs because the proposed MC^3 applies RGA phase which reduces the average path length and hence saves the energy consumption of the MC. As a result, the energy usage index of MC^3 is higher than those of CAERM and CSGP.

Fig. 14 shows comparison of the proposed MC^3 with the existing CSGP and CAERM algorithms in terms of recharging effectiveness (RE). The RE is defined as the coverage divided by the energy consumption of MC. Fig. 14(a) shows comparison of the RE of the three algorithms by varying the sleep threshold and sensing range of sensors. As shown in Fig. 14(a), the RE decreases with the sleep threshold of sensors. A higher sleep threshold will increase the frequency of recharging requests sent by sensors. Thus, the recharging workload of MCs is increased accordingly, leading to low RE. On the other hand, the RE increases with the sensing range of sensors. It occurs because a larger sensing range increases the coverage range of each sensor and hence achieves better coverage. In comparison, the proposed MC^3 performance is higher than the CSGP and CAERM algorithms. It occurs because the proposed MC^3 applies the RGA phase which obtains the request to the nearest charger (RNC) and shorter d-distance (SDD) advantages.

Fig. 14(b) shows comparison of the three algorithms in terms of RE by varying the density degree and the elapsed time. The density degree ranges from 1 to 4. The elapsed time

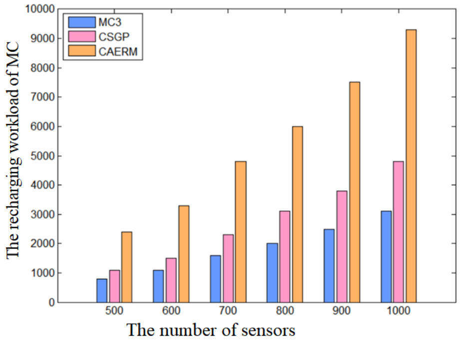

Fig. 15. Comparisons of the three algorithms in terms of recharging workload by varying the number of sensors.

is controlled ranging from 0 to 200 h. As shown in Fig. 14(b), the RE increases with the density degree of sensors. A higher density degree of sensors indicates a smaller distance between neighboring sensors. This can reduce the energy consumption of MCs, leading to a higher RE. In addition, the RE of MC^3, CSGP, and CAERM generally increases with the elapsed time. In comparison, the performance of workload balance for the MCs is higher than the CSGP and CAERM algorithms. It occurs because the applied RGA phase dynamically adjusts the MC's group, obtaining RNC and SDD advantages.

Fig. 15 illustrates comparison of the three algorithms in terms of the workload balance of MCs. As shown in Fig. 15, the recharging workload of each MC increases with the number of sensors. This is because a large number of sensors will increase the number of recharging requests, leading to higher workloads for mobile changers. It is observed that the recharging workload of CREAM is speedily increasing. This occurs because the group of MC is fixed, increasing the path length and workload of MCs. The workload of MC^3 and CSGP is slightly increasing. It occurs because they use multiple MCs to share the recharging task. The recharging workload of each MC in MC^3 is more balanced than in the CSGP algorithm. This occurs because the proposed MC^3 applies the workload balancing task. Some sensors might send the recharging request to the MCs which are not responsible for the corresponding group but have light workloads.

VI. Conclusion

This article considers the energy replenishment problem for a given WSN and proposes a cooperative charging algorithm, called MC^3, aiming to prolong the lifetime of sensor networks while improving the recharging schedule of the MCs. The proposed MC^3 partitions the network and sets the initial positions of the MCs first. Then the responsible group for each MC is changed dynamically, aiming to reduce the recharging path length and the recharging waiting time. Furthermore, each sensor selects an MC and sends a recharging request by applying the quorum system. Finally, the MC^3 schedules the recharge task while balancing the workloads of all the MCs. The analytical results show that the proposed MC^3 outperforms the existing schemes. Future work will explore sensors with adjustable sensing radius and various types of sensors in heterogeneous WSNs.

References

[1] U. Dampage, L. Bandaranayake, R. Wanasinghe, K. Kottahachchi, and B. Jayasanka, "Forest fire detection system using wireless sensor networks and machine learning," *Sci. Rep.*, vol. 12, no. 1, pp. 1–11, Jan. 2022.

[2] K. Cheena, T. Amgoth, and G. Shankar, "Proportional-integral-derivative controller-based self-healing of distribution system using wireless sensor networks in smart grid," *Int. J. Commun. Syst.*, vol. 35, no. 7, pp. 1–15, May 2022.

[3] M. Majid et al., "Applications of wireless sensor networks and Internet of Things frameworks in the industry revolution 4.0: A systematic literature review," *Sensors*, vol. 22, no. 6, p. 2087, Mar. 2022.

[4] S. M. Antony, S. Indu, and R. Pandey, "An efficient solar energy harvesting system for wireless sensor network nodes," *J. Inf. Optim. Sci.*, vol. 41, no. 1, pp. 39–50, Feb. 2020.

[5] D. K. Sah and T. Amgoth, "A novel efficient clustering protocol for energy harvesting in wireless sensor networks," *Wireless Netw.*, vol. 26, no. 6, pp. 4723–4737, May 2020.

[6] N. Qi, Y. Yin, K. Dai, C. Wu, X. Wang, and Z. You, "Comprehensive optimized hybrid energy storage system for long-life solar-powered wireless sensor network nodes," *Appl. Energy*, vol. 290, May 2021, Art. no. 116780.

[7] A. Tomar, L. Muduli, and P. K. Jana, "An efficient scheduling scheme for on-demand mobile charging in wireless rechargeable sensor networks," *Pervasive Mobile Comput.*, vol. 59, pp. 1–17, Oct. 2019.

[8] H. Guo, R. Wu, B. Qi, and Z. Liu, "Lifespan-balance-based energy-efficient routing for rechargeable wireless sensor networks," *IEEE Sensors J.*, vol. 21, no. 24, pp. 28131–28142, Dec. 2021.

[9] D. Prasannababu and T. Amgoth, "Joint mobile wireless energy transmitter and data collector for rechargeable wireless sensor networks," *Wireless Netw.*, vol. 28, no. 8, pp. 3563–3576, Aug. 2022.

[10] J. Xu, S. Hu, S. Wu, K. Zhou, H. Dai, and L. Xu, "Cooperative charging as service: Scheduling for mobile wireless rechargeable sensor networks," in *Proc. IEEE 41st Int. Conf. Distrib. Comput. Syst. (ICDCS)*, Jul. 2021, pp. 685–695.

[11] Z. Wei, M. Li, Q. Zhao, Z. Lyu, S. Zhu, and Z. Wei, "Multi-MC charging schedule algorithm with time windows in wireless rechargeable sensor networks," *IEEE Access*, vol. 7, pp. 156217–156227, 2019.

[12] K. Wang, L. Wang, C. Lin, and M. Obaidat, "Prolonging lifetime for wireless rechargeable sensor networks through sleeping and charging scheduling," *Commun. Syst.*, vol. 33, no. 8, pp. 1–21, May 2020.

[13] G. Han, H. Wang, H. Guan, and M. Guizani, "A mobile charging algorithm based on multicharger cooperation in Internet of Things," *IEEE Internet Things J.*, vol. 8, no. 2, pp. 684–694, Jan. 2021.

[14] W. Xu, W. Liang, X. Jia, Z. Xu, Z. Li, and Y. Liu, "Maximizing sensor lifetime with the minimal service cost of a mobile charger in wireless sensor networks," *IEEE Trans. Mobile Comput.*, vol. 17, no. 11, pp. 2564–2577, Nov. 2018.

[15] T. Liu, B. Wu, S. Zhang, J. Peng, and W. Xu, "An effective multi-node charging scheme for wireless rechargeable sensor networks," in *Proc. IEEE Conf. Comput. Commun.*, Aug. 2020, pp. 2026–2035.

[16] C.-Y. Chang, Y.-W. Kuo, P. Xu, and H. Chen, "Monitoring quality guaranteed barrier coverage mechanism for traffic counting in wireless sensor networks," *IEEE Access*, vol. 6, pp. 30778–30792, 2018.

[17] K. N. Qureshi, M. U. Bashir, J. Lloret, and A. Leon, "Optimized cluster-based dynamic energy-aware routing protocol for wireless sensor networks in agriculture precision," *J. Sensors*, vol. 2020, pp. 1–19, Jan. 2020.

[18] H. Yu, C.-Y. Chang, Y. Wang, D. S. Roy, and X. Bai, "CAERM: Coverage aware energy replenishment mechanism using mobile charger in wireless sensor networks," *IEEE Sensors J.*, vol. 21, no. 20, pp. 23682–23697, Oct. 2021.

[19] S. Priyadarshani, A. Tomar, and P. K. Jana, "An efficient partial charging scheme using multiple mobile chargers in wireless rechargeable sensor networks," *Ad Hoc Netw.*, vol. 113, Mar. 2021, Art. no. 102407.

[20] B. Dande, C.-Y. Chang, C.-H. Kuo, and D. Sinha Roy, "RS-STQ: Recharge scheduling algorithm for maximizing spatial and temporal data accuracy," *IEEE Sensors J.*, vol. 22, no. 23, pp. 23565–23580, Dec. 2022.

[21] B. Dande, C.-Y. Chang, S.-J. Wu, and D. S. Roy, "WLARS: workload-aware recharge scheduling mechanism for improving surveillance quality in wireless rechargeable sensor networks," *IEEE Sensors J.*, vol. 23, no. 11, pp. 12237–12250, Jun. 2023.